

**Quantifying the release of base metals from source rocks for volcanogenic
massive sulfide deposits: effects of protolith composition and alteration
mineralogy**

Simon M Jowitt^{1,2*}, Gawen R T Jenkin¹, Laurence A Coogan³ and Jon Naden⁴

¹*Department of Geology, University of Leicester, University Road, Leicester, UK, LE1 7RH*

²*School of Geosciences, Monash University, Melbourne, Australia, VIC 3800*

³*School of Earth and Ocean Sciences, University of Victoria, BC, Canada, V8W 3V6*

⁴*British Geological Survey, Kingsley Dunham Centre, Keyworth, UK, NG12 5GG*

Phone +61399053832

Fax +61399054903

e-mail: simon.jowitt@monash.edu

Abstract

This detailed study of the release of base metals during hydrothermal alteration from the sheeted dike complex of the Troodos ophiolite, Cyprus, aims to better understand the source of these elements in ore-forming hydrothermal fluids. The study area, ~10 km² between the villages of Spilia and Kannavia, has previously been recognized as a region in which the abundance of epidote in the altered sheeted dikes is higher than average – a so-called epidosite zone. The originally basaltic to andesitic sheeted dikes have been variably altered, but the secondary mineralogy is independent of the protolith composition. Four alteration facies have been identified in the epidosite zone. With progressively increasing modal epidote, decreasing modal amphibole, and decreasing bulk-rock Mg these are: (i) diabase, which is composed of amphibole + chlorite + albitic plagioclase ± epidote ± quartz, (ii) transitional diabase–epidosite, (iii) intermediate epidosite, and (iv) rare (<15% of the study area) end-member epidosite which consists largely of quartz + epidote. Comparing protolith base metal differentiation trends, defined by new analyses of cogenetic volcanic glass, with these altered samples indicates that the rocks originally contained 47–99 ppm Zn, 1030–1390 ppm Mn, 19–28 ppm Co, 19–57 ppm Cu and 7–50 ppm Ni. The vast majority of the altered rocks within the epidosite zone studied have low Cu (averaging 3 ppm) irrespective of alteration facies. This uniform and large depletion suggests that Cu was originally largely present in sulfides that were completely destroyed during hydrothermal alteration. With the exception of Co, the other base metals have substantially lower concentrations in the altered rocks than in their protoliths and show increasing base metal depletion with increasing modal epidote abundance. This suggests that breakdown of silicate minerals was important in controlling the release of these metals. Cobalt is enriched in the diabase and transitional diabase–epidosite alteration facies, and depleted in the end-member epidosite alteration facies, relative to protolith concentrations. This suggests that Co was

redistributed within the sheeted dike complex rather than substantially leached out; the same is probably true of Mg. Mapping across the steep topography of the study area indicates that the Spilia–Kannavia epidosite zone has a volume of $\sim 2 \text{ km}^3$. Based on this estimate, hydrothermal fluids leached $\sim 369 \text{ kt}$ of Zn, $\sim 52 \text{ kt}$ of Ni, $\sim 3647 \text{ kt}$ of Mn and $\sim 162 \text{ kt}$ of Cu. These Zn and Cu losses are similar to the masses of these metals present in the largest volcanogenic massive sulfide deposits on Cyprus. Based on the differences between protolith and altered rock compositions it is predicted that alteration of primitive protoliths will tend to produce fluids with higher ratios of Cu and Ni to Zn and Mn, whereas alteration of more evolved protoliths will produce fluids with lower ratios.

Keywords: *Troodos ophiolite, VMS, epidosite, hydrothermal alteration, source rocks*

1. Introduction

Understanding the relationship between source-rocks and ophiolite-hosted Volcanogenic Massive Sulfide (VMS) deposits is important both for future mineral exploration and to increase our understanding of ocean floor hydrothermal processes and chemical fluxes into the ocean. Models for hydrothermal systems at divergent plate boundaries with intermediate- to fast-spreading rates suggest that most high-temperature hydrothermal alteration occurs within the sheeted dike complex (e.g. Alt et al., 1996). Based on this, a number of studies have attempted to understand the leaching of base metals from the sheeted dike complex. For example, experimental studies have demonstrated the important role temperature can play in controlling the relative amounts of different base metals released during alteration into hydrothermal fluids and have emphasized the importance of metal sulfide solubility (e.g., Seewald and Seyfried, 1990). Studies of both modern oceanic crust and ophiolites have demonstrated that sheeted dikes are commonly depleted in at least some base metals, supporting the idea that these are source rocks for metals in VMS deposits (e.g., Alt et al., 1996; Gillis, 2002; Gillis et al., 2001; Richardson et al., 1987; Schiffman and Smith, 1988; Schiffman et al., 1987). However, different VMS deposits within the same ophiolite can have quite diverse base metal ratios and grades, and the role of source rock initial composition, and secondary mineralogy within the source region in controlling this variability, has received little study (e.g., Doe, 1994).

While the general model of leaching of metals from the sheeted dike complex by hot fluids, and subsequent deposition of some fraction of these metals in near seafloor ore bodies, is fairly well established, quantification of the mass balance involved is in its infancy. Simple mass balance calculations, based on the average compositions of fresh rocks and altered rocks, have been performed, demonstrating that alteration of sheeted dikes is a likely origin of the metals in VMS deposits (e.g., Humphris and Cann, 2000; Richardson et al., 1987).

However, there has been little attention given to the variability of the protolith composition in these calculations. This is important for two reasons. Firstly, the concentration of base metals in the protolith varies as a function of the extent of magmatic differentiation, especially for elements such as Ni with bulk partition coefficients far from unity. Secondly, protoliths with different major element compositions may alter to distinct secondary mineral assemblages, and thus release metals to the hydrothermal fluid differently.

In this study we have undertaken the most detailed investigation to-date of the distribution of base metals in both protoliths, and altered dikes, in the Troodos ophiolite, Cyprus, in order to better understand the release of base metals into hydrothermal systems associated with Cyprus-type VMS mineralization. An epidosite zone was selected for a detailed study of base metal release from the sheeted dike complex because these zones: (i) have been proposed to play a critical role in supplying base metals to the fluids that form VMS deposits (e.g., Richardson et al., 1987; Schiffman and Smith, 1988; Schiffman et al., 1987), and (ii) contain the full range of secondary mineral assemblages observed in the sheeted dike complex of the Troodos ophiolite. Thus, samples from epidosite zones allow the role of secondary mineralogy in base metal release during hydrothermal alteration to be investigated. We define protolith compositions using new Laser Ablation–Inductively Coupled Plasma–Mass Spectrometry (LA–ICP–MS) analysis of volcanic glasses from cogenetic pillow lavas to model magmatic differentiation trends for the base metals, relative to the immobile element Y. By means of an extensive suite of altered sheeted dikes, with variable secondary mineralogy, we then quantify the release of base metals from these samples and investigate how the protolith and secondary mineralogy impact this. These results also allow the bulk metal release from a given volume of rocks to be determined and compared to the mass of metals within Troodos VMS deposits.

2. Geology

2.1. *The Troodos ophiolite and its VMS deposits*

The Troodos ophiolite is a type locality for on-land studies of the upper ocean crust. It formed in a Cretaceous supra-subduction zone setting (Mukasa and Ludden, 1987; Robinson et al., 1983), and thus, unlike oceanic crust formed at modern mid-ocean ridges, the upper crust of the ophiolite is broadly basaltic andesite in composition (ranging from picritic basalts to rhyolites; e.g., Robinson et al., 1983). The ophiolite hosts 41 exploited VMS deposits that are up to ~20 Mt in size and vary from deposits with little or no base metals, that were mined for sulfur (e.g., Kokkinopezoula: 3.5 Mt at 24 wt% S and 0.2 wt% Cu, and Kambia: 1.5 Mt at 30 wt% S), to base metal rich deposits (e.g., Mavrovouni: 15 Mt at 3.8 wt% Cu, 0.5 wt% Zn; Skouriotissa: 5.4 Mt at 2.3 wt% Cu, 0.06 wt% Zn, and Kinousa: 0.3 Mt at 2.4 wt% Cu and 3.4 wt% Zn; Hannington et al., 1998). Although comparatively small on a world scale, the economic importance of these deposits is in many ways subsidiary to their value in terms of understanding mineralization processes.

2.2 *Previous work addressing base metal release from the Troodos sheeted dike complex*

A primary focus of previous work on metal leaching from the sheeted dike complex in the Troodos ophiolite has been on the role of epidotes as source rocks (e.g., Bettison-Varga et al., 1992; Richardson et al., 1987; Schiffman and Smith, 1988; Schiffman et al., 1987). These are equigranular epidote + quartz + titanite ± chlorite ± Fe–Ti-oxides (magnetite ± ilmenite) rocks with no trace of an igneous texture. These contrast with the diabase¹ dikes that make up most of the sheeted dike complex. These are amphibole + albitic plagioclase + chlorite ± epidote ± quartz ± Fe–Ti-oxides ± titanite rocks that retain an igneous texture and

¹ We follow Richardson et al. (1987) in using the term diabase to describe this alteration facies.

contain rare relics of igneous clinopyroxene. Epidosite alteration is commonly partial within any single dike (see Wilson, 1959), with stripes of epidosite parallel to the dike margins being common (e.g., Figs. 2 and 3 in Richardson et al., 1987). The remaining dike is generally less epidote-rich, tending towards the mineralogy of diabase, although chlorite-rich dikes are also commonly associated with epidosites (Richardson et al., 1987). Base metal concentrations in epidosites are substantially lower than in presumed protoliths; this has led to a genetic link between epidosites and the overlying VMS deposits being hypothesized (e.g., Humphris and Cann, 2000; Richardson et al., 1987; Schiffman et al., 1987).

Epidosites occur in abundance in zones that commonly occur near the dike–gabbro boundary, with rarer occurrences in the inter-epidosite zone regions that are dominated by diabase (Bettison-Varga et al., 1992; Richardson et al., 1987). Six zones in which epidosite alteration is common were reported by Richardson et al. (1987); five in the sheeted dike complex, including two in the Spilia–Kannavia area, and one in a plagiogranite (Fig. 1B). These zones are generally elongated parallel to the strike of the sheeted dike complex and, according to Schiffman and Smith (1988), have maximum dimensions of ~3 km by ~15 km, although it is unclear whether the epidosite zone they describe is one continuous epidosite zone or the intersection of many zones spread across differing ‘stratigraphic’ levels. Epidosite zones are known from a number of other ophiolites such as Solund–Stavfjord, Josephine, Oman and Pindos (Fonneland-Jorgensen et al., 2005; Harper, 1995; Nehlig et al., 1994; Valsami and Cann, 1992). They have also been found in the active Tonga forearc, suggesting that epidosites form in modern supra-subduction zone hydrothermal systems (Banerjee and Gillis, 2001; Banerjee et al., 2000). However, they have not been found at normal mid-ocean ridges, suggesting that epidosite formation is limited to certain tectonic environments (Banerjee and Gillis, 2001; Banerjee et al., 2000).

2.3. Geology of the study area

The Spilia–Kannavia epidosite zone, on the northern flank of the Troodos ophiolite (Fig. 1A), was selected for detailed mapping and sampling in part because the >500 m of variation in elevation allows better estimation of the volume of the epidosite zone than in flatter lying areas. Additionally, two closely spaced epidosite zones had previously been identified in this area (Richardson et al., 1987), and new mapping (Fig. 1A) demonstrates that these are linked, making a single epidosite zone. This epidosite zone lies entirely within the sheeted dike complex with no evidence of epidosite development in the subjacent plutonic rocks. There is also no evidence of increasing abundance of epidosite-altered dikes near to the plutonic–dike boundary, as has been suggested elsewhere (Bettison-Varga et al., 1992). The boundary between epidosite zone and normal sheeted dike complex lithologies is gradational over ≤ 50 m as previously noted (Richardson et al., 1987; Schiffman and Smith, 1988). This boundary is marked by a large number of small (2–5 cm wide) dike-parallel epidote–quartz veins before passing into epidosite-free diabase. Overall the epidosite zone has a maximum extent of ~5 km parallel to dike strike and ~2 km across strike (Fig. 1A), and has a maximum thickness of ~400 m, suggesting a volume of $\sim 2 \text{ km}^3$, assuming a trapezoidal cross section.

In the field the dikes were divided into two alteration facies; epidosite and diabase. Subsequent microscopy subdivided these into four facies on the basis of secondary mineralogy. In order of increasing modal epidote and decreasing modal amphibole these are termed: (i) diabase, (ii) transitional diabase–epidosite, (iii) intermediate epidosite, and (iv) end-member epidosite. *Diabase* is made up of amphibole + albitic plagioclase + chlorite \pm epidote \pm quartz \pm Fe–Ti-oxides \pm titanite and retains an igneous texture (e.g., elongate plagioclase laths that have been albitised). Clinopyroxene and, to a lesser extent, plagioclase, are replaced by amphibole (<30%), chlorite (15–30%) and minor epidote. Igneous magnetite

and ilmenite are patchily replaced by titanite. Very rare pyrrhotite and pyrite are present in a small number of samples and these were the only sulfides observed in this study. *Transitional diabase–epidosite* contains the same mineral assemblage as diabase but has a higher abundance of chlorite (>30%), epidote (15–30%) and quartz (15–30%) and lesser amphibole (<15%) and plagioclase (<15%). This alteration facies also generally lacks an igneous texture. *Intermediate epidosite* is marked by the near absence of amphibole and plagioclase, and >30% epidote and quartz with 15–30% chlorite. *End-member epidosite* consists almost entirely of epidote (up to 63%, as documented in other studies, e.g., Schiffman et al., 1990) and quartz, with <10% chlorite. Accessory titanite and Fe–Ti-oxides occur through all alteration facies with the former more abundant in epidote-rich lithologies. In the field, end-member epidosites have a spectacular pistachio green color and are less fractured than the other facies.

An estimate of the proportion of each alteration facies within the study area is required if the total amounts of base metals released from this area are to be quantified. Kilometer-scale traverses along well-exposed road sections cutting through the study area (Transects A–E in Fig. 1A) were used to estimate the proportions of the two facies identifiable in the field. These gave between 40% and 83% diabase (which includes transitional diabase–epidosite) and between 17% and 60% epidosite (which includes intermediate epidosite). When these are combined with further mapping within the epidosite zone, an average of 48% diabase and 52% epidosite is estimated overall. To quantify the proportions of the four alteration facies more accurately, two short traverses were sampled every ~10–15 cm, wherever the lithology appeared different, generally avoiding lithological boundaries and veins, with subsequent microscopy used to determine the proportions of each lithology. Samples were examined using a binocular microscope on a cut surface and thin sections were made of a subset of samples as a check on the accuracy of lithological

determinations; in >95% of cases the cleaned and cut samples were assigned correctly. The longer of these, a 4.8 m transect (SpKB), is composed of 24% diabase, 41% transitional diabase–epidosite, 30% intermediate epidosite and 5% end-member epidosite. The shorter, 1.5 m traverse (SpKA), is composed of 63% diabase, 11% transitional diabase–epidosite, 7% intermediate epidosite and 15% end-member epidosite. Weighting the lithological proportions from these short traverses by their respective lengths gives 33% diabase, 34% transitional diabase–epidosite, 25% intermediate epidosite and 8% end-member epidosite. Using these relative proportions, the 48% diabase field classification is subdivided into 24% diabase and 24% transitional diabase–epidosite. Likewise the 52% epidosite is subdivided into 39% intermediate epidosite and 13% end-member epidosite.

3. Analytical techniques

Whole-rock samples were crushed in an agate mill and analyzed for major and trace elements by X-ray Fluorescence spectrometry (XRF) and ICP–MS (Jowitt, 2009). XRF analysis at the University of Leicester used a Philips PW1400 instrument and fused glass beads for major element determinations and pressed powder pellets for trace elements. Further trace element analyses were performed using a VG Elemental PQ2 ICP–MS instrument at the British Geological Survey, Keyworth, after digesting the rock powder in a HF–HNO₃–HClO₄ mix. Analysis of standards demonstrates that Mn, Zn, Ni and Y abundances are more accurately determined by XRF whereas Co and Cu are better by ICP–MS (Jowitt, 2009); as such, these are the sources of data used throughout this study.

Fresh volcanic glass was hand-picked, mounted in epoxy resin, polished and examined by SEM to identify devitrification- and crystal-free regions for analysis. Major elements were analyzed by electron probe microanalysis (EPMA) using a JEOL 8600

Superprobe at the University of Leicester with a 30 μm spot size, 30 nA beam current and a 15 kV acceleration voltage (Jowitt, 2009). Trace element compositions were determined by LA-ICP-MS analysis using the same ICP-MS instrument used for solution analysis and a New Wave 266 nm Nd-YAG laser focused on a 40 μm spot and pulsing at a frequency of 4 Hz. Calibration, after gas blank and drift correction, was performed against BHVO-2G glass that has a similar major and trace element composition to Troodos volcanic glasses, using Ca as the internal standard. Each glass composition is the average of three replicate analyses. Further details of the analytical techniques are available in Jowitt (2009).

4. Geochemistry

4.1. Protolith compositions

Although no spatially proximal fresh protolith material exists within the sheeted dike complex, the cogenetic nature of the sheeted dike complex and overlying pillow lavas means that fresh volcanic glass within the lavas can be used to define protolith compositions. Glass provides the most reliable record of protolith compositions in nearly aphyric rocks, as found in the majority of Troodos dikes. Glass samples were collected from the lava section on the northern flanks of the Troodos ophiolite (Fig. 1B; Supplementary data Table A.1) and were used to define differentiation trends. A variety of samples (pillow rims, hyaloclastites and dike margins) from each site were sampled where possible. Changes in protolith base metal contents as a function of the concentration of the immobile element Y were determined from differentiation trends defined by the volcanic glass. Yttrium was used as the immobile element to define the degree of differentiation of the parental magma because it is fairly constant in abundance in the parental melts to the Troodos lavas, its behavior during

differentiation is relatively straightforward (e.g., unlike Ti it is not influenced by Fe–Ti-oxide saturation), and it is highly insoluble in hydrothermal fluids (e.g., Bau and Dulski, 1999).

Assuming that the glass compositions define a differentiation trend from a single parental composition, and that the distribution coefficients remain constant during differentiation, a least squares regression in the form of power law curve (Eq. 1) should reproduce the variation in base metal concentrations at differing concentrations of yttrium.

$$M_e = AY^B \quad (1)$$

where M_e is the estimated base metal content of a sample for a given yttrium concentration (Y) and A and B are regression coefficients (Table 1). The fit of the volcanic glass data to the differentiation model was quantified by determining the Root Mean Square of Deviations (*RMSD*) between the model and the data (Eq. 2).

$$RMSD = \sqrt{\frac{\sum (M_e - M_g)^2}{n}} \quad (2)$$

where M_e is the calculated base metal concentration at the measured yttrium concentration from Eq. 1, M_g is the measured base metal concentration in the glass and n is the number of samples used to define the model (Table 1).

The glass data show that during differentiation (increasing Y ; Fig. 2) the concentrations of Ni, Co and Cu decrease (compatible behavior), whereas Zn and Mn concentrations increase (incompatible behavior). This has the important implication that the extent of differentiation of the magma before dike emplacement will affect the base metal

content of the source rocks. In particular, the ratios of incompatible to compatible base metals will be substantially affected by the extent of differentiation of the parental magma.

4.2. Mass changes during alteration

The models described above show how base metal contents in the magmas that formed the sheeted dike complex may have varied with magmatic differentiation (i.e., increasing Y concentration). Thus, using the Y content as a marker of the extent of differentiation we can estimate the difference in base metal content between protolith and altered rock. For example, it could be predicted that a diabase with 30 ppm Y and 15.5 ppm Zn was derived from a protolith with 70.7 ppm Zn ($M_{Zn} = 8.1 * Y^{0.6372}$ from Eq. 1; Table 1), suggesting that, during alteration, 55.2 ppm Zn was released from the protolith. However, this approach of using Y concentration in altered rocks to estimate base metal release does not account for changes in mass associated with alteration. Assuming that Y is perfectly immobile, mass addition will lead to a dilution of Y and vice versa. Thus, large mass changes could significantly affect the modeling of base metal release.

Two lines of reasoning suggest that on a large (outcrop) scale there was little change in the mass of rock and, thus, the overall metal budget calculations are not significantly compromised by dilution/concentration effects:

- (i) Maximum mass fluxes can be estimated, using modern mid-ocean ridge hydrothermal systems as an analogue. Here, the maximum water/rock mass ratio through the sheeted dike complex is constrained by the available heat and is <4, and best-estimate water/rock ratios are 1 (e.g., Coogan and Dosso, 2012). Hydrothermal fluids generally have very similar solute contents to seawater with the bulk crust gaining a small amount of mass, largely in the form of H₂O and anhydrite (~1.2 wt%; Coogan and Dosso, 2012).

(ii) Mass changes can also be investigated by comparing the measured abundance of an immobile compatible element in an altered rock with its abundance predicted by a protolith differentiation model (Eq. 1). Here, using the fresh volcanic glass data for Y (an immobile incompatible element) and Al (an immobile compatible major element), the original Al content of an altered rock with a given Y concentration (ppm) can be estimated using the following linear relationship:

$$\text{Al}_2\text{O}_3 \text{ (wt\%)} = -0.0558*Y + 16.866 \quad (3)$$

derived from regressing Y and Al_2O_3 variation in the glass data (Supplementary data Table A.1; Given that Al is a major element, a linear relationship was used to model Al_2O_3 concentrations as power law relationships are not expected for major elements). The difference in compatibility between Y and Al leads to increases in Y being accompanied by decrease in Al during differentiation. In contrast, mass changes due to alteration will impact these immobile elements in the same sense (diluted or concentrated). Thus, mass changes will lead to large differences between the measured Al content ($\text{Al}_2\text{O}_{3\text{meas}}$) in a given sample and the Al content predicted from the Y content ($\text{Al}_2\text{O}_{3\text{protolith}}$). Using this approach the percentage mass change ($\text{Al}_2\text{O}_{3\text{change}}$) can be calculated for any single sample:

$$\text{Al}_2\text{O}_{3\text{change}} = 100*[(\text{Al}_2\text{O}_{3\text{meas}} - \text{Al}_2\text{O}_{3\text{protolith}})/\text{Al}_2\text{O}_{3\text{protolith}}] \quad (4)$$

Averaging the $\text{Al}_2\text{O}_{3\text{change}}$ value across all alteration types indicates a mean mass change during alteration of 3.62% (i.e., ~0.5 wt% Al_2O_3), only slightly higher than the 1.64% uncertainty (calculated using Eq. 2) on the modeled protolith Al_2O_3

concentrations determined using equation 3. Again, this mass change is insignificant relative to the changes in base metal concentrations during alteration (Table 2).

Based on the assumption that Y is immobile, and given that the total mass change in the epidosite zone is small, mass addition and removal are likely to have had minimal effect on the total metal budgets we calculate.

4.3. Sheeted dike complex geochemistry

In addition to detailed sampling along the two short traverses described above, samples were collected throughout the epidosite zone (Fig. 1A). In total 137 samples were collected from the Spilia–Kannavia epidosite zone and analyzed for bulk-rock geochemistry (Supplementary data Table A.2). These comprise 62 diabase, 26 transitional diabase–epidosite, 31 intermediate epidosite and 18 end-member epidosite samples.

The major element compositions of the sheeted dikes largely reflect the variation in mineralogy, with increasing modal epidote associated with increased Ca and Si and decreased Na, K and Mg concentrations relative to protolith (see Richardson et al., 1987; Schiffman et al., 1990). The bulk epidosite zone lies on the differentiation trend defined by the volcanic glasses in Si–Ca–Mg–Al–K composition space but is depleted in Na relative to the glasses. Importantly, there does not appear to be any systematic difference in the protoliths for the different alteration facies, based on the concentrations and ratios of immobile elements (e.g., Y and Ti; Fig. 2f). This indicates that how evolved the dike was had little or no impact on the subsequent style of alteration. This is consistent with significant variation in secondary mineralogy within single dikes that presumably had the same protolith composition.

Using the measured Y content of the altered dikes, and the protolith differentiation models derived from the glass data (Table 1), protolith base metal contents (M_e) can be determined for each sample. From this, we estimate that the protoliths contained 47–99 ppm

Zn, 1030–1390 ppm Mn, 19–28 ppm Co, 19–57 ppm Cu and 7–50 ppm Ni. Dikes within the Spilia–Kannavia epidosite zone generally have much lower concentrations of Cu, Zn, Ni and Mn than these protolith values (Fig. 2). The extent of base metal depletion is similar across all alteration facies for Cu but increases with increasing modal epidote for Ni and, to a lesser extent, Zn and Mn (Fig. 2). In contrast to the other base metals, Co is enriched in amphibole- and chlorite-rich lithologies (diabase and transitional diabase–epidosite) and only depleted in end-member epidosites. While some of this may reflect uncertainty in defining the parental melt Co content, it seems that Co is redistributed between rocks with different secondary mineralogies rather than being lost from the epidosite zone as a whole as discussed below.

In comparison to the modeled protolith compositions and within a given alteration facies,, it is found that dike compositions are more or less independent of protolith composition, and base metal contents do not parallel protolith metal contents but are instead more or less independent of protolith composition. This means that more evolved rocks, with higher protolith Zn, Mn and Y but lower Ni and Cu, have generally lost more Zn and Mn and less Ni and Cu.

The two detailed sampling traverses allow the impact of variable secondary mineralogy on base metal behavior to be investigated on a local scale (Figs. 3 and 4). Both traverses show substantial variation in base metal concentration over short distances that broadly correlate with the alteration facies as observed over the entire study area. This relationship with alteration mineralogy leads to strong correlations between bulk-rock MgO (controlled largely by the modal abundance and composition of chlorite and amphibole) and Zn, Co and Mn concentrations (Fig. 5). Local redistribution of elements is suggested by enrichment of Mg, Ni, Co and, to a lesser extent, Zn and Mn in the diabase immediately surrounding the main zone of end-member epidosite in traverse SpKA (Fig. 3). Similar small-scale variations are not evident in traverse SpKB (Fig. 3) due to the shorter distances over

which lithologies are inter-mixed. Notably, there are large variations in Mg on a decimeter-scale in both traverses, indicating variations in the abundance of chlorite \pm amphibole. The variability of Mg is consistent with the observation of Richardson et al. (1987) that epidiosites are commonly associated with chlorite-rich lithologies. The small scale of mineralogical and chemical variation suggests that the hydrothermal fluids would have had their compositions buffered by reactions with a large number of phases, rather than an external fluid controlling the phase equilibria through extremely high fluid-fluxes (e.g., Seyfried et al., 1988).

4.4. Base metal release from the Spilia–Kannavia epidosite zone

The method we used to determine changes in base metal concentrations during alteration uses the protolith base metal concentrations determined in Section 4.1. The approach of using less altered cogenetic pillow lavas as a protolith for sheeted dike complex lithologies has been used on the Troodos ophiolite before (e.g. Richardson et al. 1987; Cowan, 1989; Humphris and Cann, 2000). However, these studies have used a single protolith composition rather than a different protolith composition for each sample as used here. Additionally, previous studies have used weakly altered pillow lava material as a protolith rather than entirely fresh volcanic glass as we do here.

As both lavas and sheeted dikes are compositionally variable due to differing degrees of igneous differentiation, it is not possible to define a single protolith for the entire sheeted dike complex, as for example used in the Gresens' method for calculating compositional changes during alteration (Grant, 1986, 2005). Instead, we modeled the base metal concentration in the protolith for each sample (Fig. 2; Eq. 1; Table 1) and compared this to measured altered sheeted dike compositions. The immobile element yttrium is used to define the extent of differentiation (Eq. 1). This enables the estimation of the original base metal concentrations within individual dike samples, and thus the concentration of base metals lost

during alteration. This methodology ensures that, by modeling protolith concentrations for each individual sample rather than selecting an average protolith, and by tailoring modeled protolith curves to the study area rather than using a more general protolith curve, we can increase the accuracy of our estimation of the amount of base metal mobilized during epidosite zone alteration in the Troodos ophiolite.

The changes in metal content (ΔM) between *each* altered rock (M_{alt}) and the modeled protolith curve at the same concentration of Y as the altered rock (M_e) were calculated using equation 5; a graphical representation of this calculation is shown by the two arrows in Fig. 2a.

$$\Delta M = M_{alt} - M_e \quad (5)$$

Statistics for ΔM values were then calculated for each alteration facies (Table 2; Fig. 6).

The calculated ΔM values for individual samples vary as a function of both secondary mineralogy, as evidenced by generally lower Zn, Mn, Co and Ni concentrations in end-member epidosites when compared to other altered rocks (Fig. 2), but also as a function of the original concentration in the protolith. This can be seen in Fig. 2a, where ΔZn values across all facies are generally smaller at lower Y concentrations (as shown by the Y = 25 ppm arrow) than at higher Y contents (e.g., 45 ppm Y), primarily due to the higher original concentration of Zn within the protolith.

The methodology used to determine ΔM values during this study is further explored in Fig. 7, which shows the relationship between protolith concentration and ΔM using a nominal altered rock Ni content. Consider an altered rock with a Y concentration of 20 ppm (indicated by a circle). This would have a Ni concentration of 7.5 ppm (i.e., M_{alt}). The modeled protolith composition at this Y concentration is 34.1 ppm, (M_e , shown as a square) giving a ΔNi value

for this hypothetical sample of -26.6 ppm, or a loss of 78% of the original Ni content. This contrasts with the much greater Ni loss if the sample was more primitive (up to -83 ppm) and much smaller Ni loss if the sample was highly evolved (down to -4 ppm). Our approach also takes into account the range of protolith compositions within the Spilia–Kannavia epidosite zone, something that is *not* considered if an approach where *only* average protolith and average altered rock Ni concentrations (Table 3) were used.

To convert the volume of each alteration facies to mass, rock densities from Cowan (1989) were used; 2847 kg m⁻³ for diabase and transitional diabase–epidosite, and 3095 kg m⁻³ for intermediate epidosite and end-member epidosite, respectively. Using these data, the estimated volume (2 km³), the proportions of the different alteration facies, and the average change in metal concentrations for each alteration facies (Fig. 6; Table 2), the total metal loss from the Spilia–Kannavia epidosite zone can be determined (Table 4, Fig. 8). The total amount of Zn, Ni, Mn and Cu released by the diabase, transitional diabase–epidosite and end-member epidosite facies are similar, with somewhat more released by the intermediate epidosite facies, largely due to its greater abundance. Cobalt was apparently redistributed within the epidosite zone rather than leached from it, with increases in Co concentration in diabase and transitional diabase–epidosite and decreases in Co concentration in the end-member epidosite facies (Fig. 6). The overall slight increase in Co across the entire epidosite zone (42 ± 27 kt; Table 4) is not considered significant based on the uncertainty in the protolith differentiation trend. In MORB suites, Co appears to show a change in behavior in the melt during crystallization at an MgO content of ~6 wt%, from either increasing, or staying constant, during initial differentiation ($K_d \leq 1$), to becoming depleted during further crystallization ($K_d > 1$). While differentiation of the Troodos magmas was different to that of MORB, this suggests that a change in the crystallizing assemblage can substantially impact

the bulk partition coefficient for Co, and thus our simple fit to the glass data may underestimate the Co content of the protolith in the more primitive (low Y) samples.

5. Discussion

5.1. Comparison of the metal loss from the Spilia–Kannavia epidosite zone and the metal content of cogenetic VMS deposits

Comparison of the amounts and relative ratios of base metals released from the Spilia–Kannavia epidosite zone can now be made with those in Cyprus-type VMS deposits. Our estimates suggests that, in total, hydrothermal fluids leached ~369 kt of Zn, 52 kt of Ni, 3647 kt of Mn and 162 kt of Cu from the Spilia–Kannavia epidosite zone (Table 4; Fig. 8). There are few data for comparison with these figures on the Ni and Co content of the Troodos VMS deposits. However, the amount of Cu released could form a large Troodos VMS deposit (e.g., the Phoukasa deposit, containing 125 kt Cu; P in Fig. 9A), whilst the Zn released during the formation of the Spilia–Kannavia epidosite zone exceeds that contained within any single Troodos VMS deposit (<100 kt; Fig. 9B). It should be borne in mind that not all metal leached from the sheeted dikes will be deposited near the seafloor, and even those metals that are deposited near the seafloor may be later removed by weathering and therefore not preserved. For example, much metal is vented into the ocean and then deposited in metalliferous sediments. In Cyprus, the umbers provide some insight into the composition of these sediments. These can contain up to 13 wt% Mn, 2500 ppm Cu, 400 ppm Ni, 200 ppm Co and 500 ppm Zn (Bear, 1963; Boyle, 1990; Constantinou, 1980; Prichard and Maliotis, 1998). Assuming that all the Mn leached from the Spilia–Kannavia epidosite zone ended up in umber of this composition, ~28 Mt of umber could be produced and could sequester ~70 kt

of Cu, ~11 kt of Ni, ~6 kt of Co and ~14 kt of Zn. Whilst these figures are not significant for Zn, this amounts to ~22% of the Ni and ~43% of the Cu released from the Spilia–Kannavia epidosite zone. This suggests that, during formation of the largest Cu deposits in Cyprus, Cu may have been leached from a somewhat larger region than the Spilia–Kannavia epidosite zone, or alternatively from more primitive (higher protolith Cu) source rocks.

Humphris and Cann (2000), building on the work of Richardson et al. (1987) and Cowan (1989), estimated that formation of a Troodos epidosite zone 2 km³ in size would release ~140 kt of Cu, 230 kt of Zn and 5700 kt of Mn. This is similar to our estimate for Cu but substantially higher for Mn and lower for Zn. The greater amount of Mn in their estimate largely reflects their assumption of 2000 ppm Mn in all protoliths, higher than any of the volcanic glasses analyzed in this study, or any other we know of. The lower Zn is due to their use of smaller average Zn loss (40 ppm) than we observed (>55 ppm in all lithologies); this difference may reflect spatial heterogeneity in the extent of metal loss from the sheeted dikes of the Troodos ophiolite.

Importantly, our study shows that variations in the composition of the protolith, and in the proportions of different alteration facies within a source region, will influence the total amount of metal available in hydrothermal fluids to form VMS deposits. More primitive protoliths will release relatively more Cu and Ni and less Zn and Mn into hydrothermal fluids during alteration and epidosite formation (Fig. 10). This is especially true of Cu, where the consistent amount of Cu loss during alteration, independent of facies (e.g., diabase, which lost an average of 91% Cu during alteration, versus end-member epidosite, which lost an average of 87% Cu; Table 2) means that the dominant control on the amount of Cu mobilized was the protolith concentration (Fig. 10). In turn, all other things being equal, the differences in base metal concentrations between primitive and evolved protoliths means that alteration of primitive protoliths would lead to hydrothermal fluids, and therefore potentially VMS

deposits, with higher Cu:Zn, Cu:Mn, Ni:Zn and Ni:Mn ratios, than if the source rocks were more evolved (Fig. 10). In addition, the greater the abundance of epidote, and the lesser the amounts of chlorite and amphibole, that form within the source rocks, the more Zn, Ni and Mn will be released into ore-forming fluids (Fig. 6). In contrast, irrespective of the mineralogy of the source region, Cu-rich fluids will always be released during alteration of the sheeted dike complex.

5.2. Mineralogical controls on base metal release into hydrothermal fluids

It is commonly assumed that Fe, Cu and Zn concentrations in hydrothermal vent fluids at mid-ocean ridges are controlled by the solubility of sulfides (\pm magnetite) that concentrated these metals (e.g., Metz and Trefry, 2000; Seewald and Seyfried, 1990; Seyfried and Ding, 1995). For example, base metal concentrations in hydrothermal fluids may be buffered by reactions such as:



There has been less work to understand the controls on Co although it has been suggested that chalcopyrite solubility controls Co abundances (e.g., Metz and Trefry, 2000). In contrast, Mn is known to be controlled by silicate and Fe–Ti-oxide phases and does not form sulfides (e.g., German and Von Damm, 2003).

The uniform, and almost zero, Cu content of the dikes in the Spilia–Kannavia epidosite zone, irrespective of alteration facies, suggests that Cu was originally present in a sulfide phase that has been completely removed from the rocks during alteration. This is consistent with the absence of sulfides in all but a few diabase samples. This has two

important implications. Firstly, Cu-rich hydrothermal fluids, and hence potentially Cu-rich mineral deposits, were produced irrespective of the alteration mineralogy in the source rocks. Secondly, the hydrothermal fluids that reacted with these rocks after the Cu-bearing sulfide phase was completely leached out would have been Cu-depleted. These 'late' fluids would not have been capable of producing Cu-rich VMS deposits. Likewise, such fluids sampled at the seafloor today, most likely in supra-subduction zone settings (Banerjee et al., 2000), would provide misleading information if interpreted as being in equilibrium with chalcopyrite at depth in the crust. For example, the high Fe/Cu of such fluids would imply very reducing conditions within the sheeted dike complex if they were assumed to have formed in equilibrium with chalcopyrite (Seyfried and Ding, 1995).

If hydrothermal alteration completely leached the sulfides out of the sheeted dikes then the remaining base metals must be contained in other phases. The correlations of bulk-rock Co, Zn, Ni and Mn with MgO (Fig. 5) suggest that these elements are all substantially hosted in Mg-bearing silicate minerals (chlorite and/or amphibole), an interpretation supported by ion probe measurement of these phases (Jowitt et al., 2009). Thus, at least by the late stages of metal leaching, the stability of these mineral phases, not the stability of sulfides (Eq. 6), will have controlled the release of these metals into the ore forming hydrothermal fluids. The strong correlation of Co and MgO (Fig. 5), along with the lack of significant loss of either element from the epidosite zone as a whole (Fig. 6; Table 4) suggests that these elements underwent local redistribution during formation of different secondary mineral assemblages. These elements are concentrated in chlorite and amphibole-rich rocks and depleted in epidote-rich rocks. This suggests that the formation of the different alteration facies was synchronous, with the same fluid interacting with all alteration facies. This local Mg redistribution is consistent with previous reports of very chlorite-rich rocks associated with epidosites (Richardson et al., 1987). Local element redistribution is also

consistent with the close association of the different alteration facies and the enrichment of Mg and Co in the wall-rocks to end-member epidiosites (Figs. 3 and 4).

Finally we suggest caution in interpreting epidiosites as regions of extremely high water-to-rock ratios. For example, based on the amount of water needed to leach the Mg out of an end-member epidiosite, assuming a fluid with vent-fluid like Mg content, Seyfried et al. (1988) suggested water-to-rock ratios of up to ~1000. However, if Mg is simply locally redistributed from epidote-rich to chlorite-rich regions on a dm-scale then these water-to-rock ratio estimates are invalid. This suggestion is consistent with the similar Sr-isotopic composition of all alteration facies within the Troodos ophiolite (Bickle and Teagle, 1992), an observation that suggests similar water-to-rock ratios for all samples. Differences in secondary mineralogy, and not differences in water-to-rock ratios, most likely controls the varying amounts of base metals leached from different alteration facies.

6. Summary and conclusions

This detailed study of base metal leaching from the Spilia–Kannavia epidiosite zone in the sheeted dike complex of the Troodos ophiolite paid special attention to protolith compositions and secondary mineralogy. Using regressions of glass base metal concentrations against the immobile element Y to define protolith differentiation trends reveals that: (i) during hydrothermal alteration, larger amounts of the compatible elements Ni and Cu were leached from more primitive protoliths, and larger amounts of the incompatible elements Zn and Mn were leached from more evolved protoliths, and (ii) the protolith composition does not control the secondary mineral assemblage formed. Altered rock mineralogy plays a role in the amount of base metals released, with chlorite- and amphibole-

rich lithologies releasing smaller amounts of Ni, Zn and Mn than epidote-rich lithologies. Copper depletion is almost complete in all rocks and is unrelated to secondary mineralogy; this probably reflects the complete breakdown of igneous sulfides that contained almost all of the protolith Cu. The important role of silicate phases in controlling the amount of base metal released contrasts with the common assumption that metal sulfide solubility controls base metal concentrations within mineralizing fluids at depth in the crust in VMS systems. Cobalt (and Mg) is locally redistributed from epidote-rich rocks to chlorite \pm amphibole-rich rocks. The total amounts of Zn and Cu released from the $\sim 2 \text{ km}^3$ study area are similar to those found within medium to large Troodos VMS deposits. This is consistent with previous suggestions (e.g., Humphris and Cann, 2000) that, assuming efficient deposition of metals near the seafloor, source zones for these deposits are of this approximate size.

Acknowledgements

SMJ acknowledges funding and support for PhD research from the British Geological Survey University Funding Initiative (BUFI) and from the University of Leicester. Fieldwork was funded by two Society of Economic Geologists Student Research Grants, and by the Edgar Pam Fellowship and G Vernon Hobson Bequest of the Institute of Materials, Minerals and Mining. EMED Mining and Stelios Nicolaides and Zomenia Zomeni at the Geological Survey Department, Ministry of Agriculture, Natural Resources and Environment, Cyprus supplied vital logistical support during fieldwork. We thank Simon Chenery, Kay Green and Tom Barlow for assistance with solution and LA-ICP-MS preparation and analysis, Nick Marsh and Rob Kelly for assistance during XRF analysis and Rob Wilson for assistance during SEM and EPMA work. Two anonymous reviewers provided useful comments which

improved the manuscript. JN publishes with permission of the Executive Director, NERC
British Geological Survey.

ACCEPTED MANUSCRIPT

Supplementary material:

Table A.1: Glass LA–ICP–MS data

Table A.2: Whole-rock sheeted dike analyses

References

- Alt, J.C., Laverne, C., Vanko, D., Tartarotti, P., Teagle, D.A.H., Bach, W., Zuleger, E., Erzinger, J., Honnorez, J., 1996. Hydrothermal alteration of a section of upper oceanic crust in the eastern equatorial Pacific: a synthesis of results from DSDP/ODP Legs 69, 70, 83, 111, 137, 140, 148 at Site 504B, in: Alt, J.C., Kinoshita, H., Stokking, L.B., Michael, P.J. (Eds.), Proceedings of the Ocean Drilling Program, Scientific Results Volume 148. Ocean Drilling Program, College Station, Texas, pp. 417–434.
- Banerjee, N. R., Gillis, K. M., 2001. Hydrothermal alteration in a modern suprasubduction zone: The Tonga forearc crust. *Journal of Geophysical Research-Solid Earth* 106, 21737–21750.
- Banerjee, N. R., Gillis, K. M., Muehlenbachs, K., 2000. Discovery of epidiosites in a modern oceanic setting, the Tonga forearc. *Geology* 28, 151–154.
- Bau, M., Dulski, P., 1999. Comparing yttrium and rare earths in hydrothermal fluids from the Mid-Atlantic Ridge: implications for Y and REE behaviour during near-vent mixing and for the Y/Ho ratio of Proterozoic seawater. *Chemical Geology* 155, 77–90.
- Bear, L. M., 1963. The mineral resources and mining industry of Cyprus. Geological Survey Department, Nicosia, Cyprus.
- Bednarz, U., Schmincke, H. U., 1994. Petrological and chemical evolution of the northeastern Troodos Extrusive Series, Cyprus. *Journal of Petrology* 35, 489–523.

- Bettison-Varga, L., Varga, R. J., Schiffman, P., 1992. Relation between ore-forming hydrothermal systems and extensional deformation in the Solea Graben spreading center, Troodos Ophiolite, Cyprus. *Geology* 20, 987–990.
- Bickle, M.J., Teagle, D.A.H., 1992. Strontium Alteration in the Troodos Ophiolite - Implications for Fluid Fluxes and Geochemical Transport in Mid-ocean Ridge Hydrothermal Systems. *Earth and Planetary Science Letters* 113, 219–237.
- Boyle, J. F., 1990. The composition and origin of oxide metalliferous sediments from the Troodos Ophiolite, Cyprus, in: Malpas, J., Moores, E. M., Panayiotou, A., Xenophontos, C. (Eds.), *Ophiolites; oceanic crustal analogues; proceedings of the symposium "Troodos 1987"*. Ministry of Agriculture and Natural Resources, Nicosia, Cyprus, pp. 705–717.
- Constantinou, G., 1980. Metallogensis associated with the Troodos Ophiolite, in: Panayiotou, A. (Ed.), *Ophiolites; Proceedings, International ophiolite symposium*. Geological Survey Department, Ministry of Agriculture and Natural Resources, Nicosia, Cyprus, pp. 663–674.
- Coogan, L. A., Dosso, S., 2012. An internally consistent, probabilistic, determination of ridge-axis hydrothermal fluxes from basalt-hosted systems. *Earth and Planetary Science Letters* 323–324, 92–101.
- Cowan, J. G., 1989, *Geochemistry of reaction zone source rocks and black smoker fluids in the Troodos ophiolite*. Unpublished PhD thesis, University of Newcastle upon Tyne.
- Doe, B.R., 1994. Zinc, copper, and lead in mid-ocean ridge basalts and the source rock control on Zn/Pb in ocean-ridge hydrothermal deposits. *Geochimica et Cosmochimica Acta* 58, 2215–2223.
- Fonneland-Jorgensen, H., Furnes, H., Muehlenbachs, K., Dilek, Y., 2005. Hydrothermal alteration and tectonic evolution of an intermediate- to fast-spreading back-arc

- oceanic crust: Late Ordovician Solund-Stavfjord ophiolite, western Norway. *Island Arc* 14, 517–541.
- Gass, I. G., MacLeod, C. J., Murton, B. J., Panayiotou, A., Simonian, K. O., Xenophontos, C., 1994. The geology of the southern Troodos transform fault zone. Ministry of Agriculture and Natural Resources, Nicosia, Cyprus.
- German, C.R., Von Damm, K.L., 2003. Hydrothermal processes, in: Elderfield, H. (Ed.), *The Oceans and Marine Geochemistry, Treatise on Geochemistry*. Elsevier-Pergamon, Oxford, pp. 181–222.
- Gillis, K.M., Muehlenbachs, K., Stewart, M., Gleeson, T., Karson, J., 2001. Fluid flow patterns in fast-spreading East Pacific Rise crust exposed at Hess Deep. *Journal of Geophysical Research-Solid Earth* 106, 26311–26329.
- Gillis, K.M., 2002. The rootzone of an ancient hydrothermal system exposed in the Troodos ophiolite, Cyprus. *Journal of Geology* 110, 57–74.
- Grant, J. A., 1986. The Isocon Diagram – A Simple Solution to Gresens' Equation for Metasomatic Alteration. *Economic Geology* 81, 1976–1982.
- Grant, J. A., 2005. Isocon analysis: A brief review of the method and applications. *Physics and Chemistry of the Earth* 30, 997–1004.
- Hannington, M. D., Galley, A. G., Herzig, P. M., Petersen, S., 1998. Comparison of the TAG mound and stockwork complex with Cyprus-type massive sulfide deposits, in: Herzig, P. M., Humphris, S. E., Miller, J. D., Alt, J. C., Becker, K., Brown, D., Bruegmann, G. E., Chiba, H., Fouquet, Y., Gemmell, J. B., Guerin, G., Hannington Mark, D., Holm, N. G., Honnorez, J., Iturrino, G. J., Knott, R., Ludwig, R. J., Nakamura, K., Petersen, S., Reysenbach, A. L., Rona, P. A., Smith, S. E., Sturz, A. A., Tivey, M. K., Zhao, X. L., Riegel, R. N. (Eds.), *Proceedings of the Ocean Drilling Program*,

- Scientific Results Volume 158. Ocean Drilling Program, College Station, Texas, pp. 389–415.
- Harper, G. D., 1995. Pumpellyosite and prehnite associated with epidosite in the Josephine ophiolite - Ca metasomatism during upwelling of hydrothermal fluids at a spreading axis, in: Schiffman, P., Day, H. W. (Eds.), *Low-grade metamorphism of mafic rocks*, GSA Special Paper 296. Boulder, Colorado, pp. 101–122.
- Humphris, S. E., Cann, J. R., 2000. Constraints on the energy and chemical balances of the modern TAG and ancient Cyprus seafloor sulfide deposits. *Journal of Geophysical Research-Solid Earth* 105, 28477–28488.
- Jowitt, S. M., 2009. Field, petrological and geochemical constraints on the release of base metals into hydrothermal fluids in Cyprus-type Volcanogenic Massive Sulfide (VMS) systems: an investigation of the Spilia-Kannavia epidosite zone, Troodos ophiolite, Cyprus. Unpublished PhD thesis, University of Leicester. EThOS Persistent ID: uk.bl.ethos.509287; available from <http://ethos.bl.uk>
- Jowitt, S. M., Jenkin, G. R. T., Coogan, L. A., Naden, J., 2009. Quantifying the release of base metals into hydrothermal ore forming systems: A SIMS investigation of potential source rocks for ophiolite-hosted Volcanogenic Massive Sulphide systems, in: Harley, S. L. (Ed.), *Micro-Analysis, Processes, Time (MAPT)*; proceedings of the annual meeting of the Mineralogical Society. Edinburgh, UK, pp. 157–158
- Metz, S., Trefry, J. H., 2000. Chemical and mineralogical influences on concentrations of trace metals in hydrothermal fluids. *Geochimica et Cosmochimica Acta* 64, 2267–2279.
- Mukasa, S. B., Ludden, J. N., 1987. Uranium-lead isotopic ages of plagiogranites from the Troodos Ophiolite, Cyprus, and their tectonic significance. *Geology* 15, 825–828.

- Nehlig, P., Juteau, T., Bendel, V., Cotten, J., 1994. The Root Zones of Oceanic Hydrothermal Systems - Constraints from the Samail Ophiolite (Oman). *Journal of Geophysical Research-Solid Earth* 99, 4703–4713.
- Prichard, H. M., Maliotis, G., 1998. Gold mineralization associated with low-temperature, off-axis, fluid activity in the Troodos ophiolite, Cyprus. *Journal of the Geological Society* 155, 223–231.
- Richardson, C. J., Cann, J. R., Richards, H. G., Cowan, J. G., 1987. Metal-depleted root zones of the Troodos ore-forming hydrothermal systems, Cyprus. *Earth and Planetary Science Letters* 84, 243–253.
- Robinson, P.T., Melson, W.G., O'Hearn, T., Schmincke, H.-U., 1983. Volcanic glass compositions of the Troodos ophiolite, Cyprus. *Geology* 11, 400–404.
- Schiffman, P., Smith, B.M., Varga, R.J., Moores, E.M., 1987. Geometry, conditions and timing of off-axis hydrothermal metamorphism and ore-deposition in the Solea graben. *Nature* 325, 423–425.
- Schiffman, P., Bettison, L. A., Smith, B. M., 1990. Mineralogy and geochemistry of epidotes from the Solea Graben, Troodos Ophiolite, Cyprus, in Malpas, J., Moores, E. M., Panayiotou, A., Xenophontos, C. (Eds.), *Ophiolites; oceanic crustal analogues; proceedings of the symposium "Troodos 1987"*. Ministry of Agriculture and Natural Resources, Nicosia, Cyprus, pp. 673–683.
- Schiffman, P., Smith, B. M., 1988. Petrology and oxygen isotope geochemistry of a fossil seawater hydrothermal system within the Solea Graben, northern Troodos Ophiolite, Cyprus. *Journal of Geophysical Research-Solid Earth* 93, 4612–4624.
- Seewald, J. S., Seyfried, W. E., 1990. The effect of temperature on metal mobility in subsurface hydrothermal systems: constraints from basalt alteration experiments. *Earth and Planetary Science Letters* 101, 388–403.

- Seyfried, W. E., Ding, K., 1995. Phase equilibria in subseafloor hydrothermal systems: a review of the role of redox, temperature, pH and dissolved Cl on the chemistry of hot spring fluids at mid-ocean ridges, in: Humphris, S. E., Zierenberg, R. A., Mullineaux, L. S., Thompson R. E. (Eds.), *Seafloor Hydrothermal Systems: Physical, Chemical, Biologic and Geological Interactions*, Geophysical Monograph vol. 91, American Geophysical Union, Washington D.C., pp. 248–273.
- Seyfried, W. E., Berndt, M. E., Seewald, J. S., 1988. Hydrothermal alteration processes at mid-ocean ridges: constraints from diabase alteration experiments, hot-spring fluids and composition of the oceanic crust. *Canadian Mineralogist* 26, 787–804.
- Taylor, R. N., 1987. The stratigraphy, geochemistry and petrogenesis of the Troodos extrusive sequence, Cyprus. Unpublished PhD thesis, University of Southampton, United Kingdom.
- Valsami, E., Cann, J. R., 1992. Mobility of rare earth elements in zones of intense hydrothermal alteration in the Pindos ophiolite, Greece, in: Parson, L. M. (Ed.), *Ophiolites and their modern oceanic analogues*. Geological Society Special Publication 60, Geological Society, London, pp. 219–232.
- Wilson, R.A.M., 1959. The geology of the Xeros-Troodos area. Geological Survey Department Memoir Number 1, Geological Survey Department, Nicosia, Cyprus.

Figure Captions

Figure 1. (A) The Spilia–Kannavia epidosite zone and sampling locations. Water course and road information is courtesy of the Lands and Surveys Department, Cyprus, and dike–intrusive boundaries in east and south of map are taken from digital data provided by the Geological Survey Department, Cyprus. (B) The location of the Spilia–Kannavia epidosite

zone within the central Troodos ophiolite (inset) and locations where volcanic glasses were sampled within the lava sequence to define protolith compositions.

Figure 2. Base metal concentrations plotted against yttrium concentration for altered dikes and volcanic glass samples. The solid line is a power law regression through the new glass analyses used to define the protolith compositions (Eq. 1; Table 1). A few glass data that plot off the scale were also included in the regression. Increases in the concentration of Zn (a) and Mn (c) with increasing Y in the glasses indicate that these elements behaved incompatibly during igneous differentiation; decreasing Ni (b), Co (d) and Cu (e) with increasing Y in the glasses indicate compatible behavior. The much lower concentrations of Zn, Mn, Ni and Cu in the altered rocks than the glass protoliths indicate that these elements were efficiently leached from the epidosite zone. In contrast, Co does not appear to have been removed from the epidosite zone but instead simply redistributed from epidote-rich to chlorite and amphibole-rich lithologies. There is no systematic difference in the Y content of altered rocks with different secondary mineralogies (f) indicating that the protolith composition did not control the subsequent alteration. Published fresh lavas are from bulk analysis of handpicked glasses that inevitably contain some alteration products (Taylor, 1987; Gass et al., 1994; Bednarz and Schminke, 1994). The arrows in part (a) indicate the methodology used for calculating changes in base metal concentrations during alteration with equation 5, by determining the difference between the measured amount of a base metal in an individual sample and the modeled concentration of the same base metal in the protolith at the same concentration of the immobile element Y; 25 and 45 ppm Y in this example. Analyses below the detection limit are plotted at the detection limits of 3 ppm for Ni, 2.7 ppm for Zn and 1.5 ppm for Cu. Error bars show the precision of an average whole-rock analysis.

Figure 3. Variation in (a) MgO, (b) Zn, (c) Ni, (d) Mn and (e) Co contents along 1.5 m sampling traverse SpKA (Fig. 1A). Note the wide variability in MgO over small distances, largely reflecting variations in the modal abundance of chlorite and amphibole. Note also that Mg, Ni, Co and, to a lesser extent, Zn and Mn are enriched in the rocks surrounding a 30 cm zone of end-member epidosite (black arrows). This is interpreted as local transport of these elements from end-member epidosite and into the adjacent wall-rock diabase. A thin quartz vein and thin spherulitic dike (2 analyses) cut this section. Analytical precision is of the order of the symbol size. Note that the diabase containing quartz-epidote veins (circled) is not included in calculating the average composition of diabase (Table 3).

Figure 4. Variation in (a) MgO, (b) Zn, (c) Ni, (d) Mn and (e) Co concentrations along a 4.8 m traverse (SpKB; Fig. 1A). Note the small-scale variation in alteration facies along the outcrop. The dashed lines indicate dike margins defined by a region of much higher P_2O_5 concentrations and P/Y ratios between ~2.1 and 4.0 m along the section; recrystallization prevents identification of dike margins in the field. Base metal concentrations vary substantially both within and between lithologies on a small scale. Analytical precision is of the order of the symbol size.

Figure 5. MgO versus Zn, Ni, Mn and Co for samples collected along the short traverses shown in Figs. 3 and 4 with all bulk-rock dike analyses as a field. Traverse SpKA samples are shown as filled symbols and traverse SpKB samples are shown as open symbols; the shape of the symbol denotes the alteration facies. Note the strong positive correlation of MgO, a rough proxy for modal chlorite \pm amphibole, and the concentrations of all of these elements when examined on a small scale (and across the entire region for Co). These strong correlations are interpreted as indicating that these elements are largely dissolved in silicate

minerals and not accessory phases, such as sulfides and magnetite, as is commonly assumed. Analyses below detection limit are plotted at the detection limit as in Figure 2. Analytical precision is of the order of the symbol size.

Figure 6. Mean changes in base metal concentrations during alteration for individual alteration facies (Table 2).

Figure 7. Diagram showing how protolith composition affects ΔM values using the modeled Ni protolith concentration curve (grey line; Table 1) and hypothetical altered rock compositions corresponding to a loss of 78% of the Ni originally within the rock during hydrothermal alteration (black line). The diagram shows the methodology used to determine ΔNi values during this study by comparing protolith (square) and altered rock compositions (circle) with the same Y concentration. Note the wide range in ΔNi values, from -83.2 ppm at 10 ppm Y to -4.35 ppm at 60 ppm Y.

Figure 8. The amount of metal released from individual alteration facies and the total metal release during formation of the Spilia–Kannavia epidosite zone (Table 4).

Figure 9. Grade versus tonnage plots for (a) Cu and (b) Zn in Troodos VMS deposits (Hannington et al., 1998); P denotes the Phoukasa deposit. For comparison the tonnage of altered rock, and the concentration of each element lost (Table 4) from the Spilia–Kannavia epidosite zone, are shown as diamonds; note that the uncertainty on these (Table 4) is smaller than the symbol.

Figure 10. Examples of the potential importance of the protolith composition in controlling the amount of different base metal leached from sheeted dikes during alteration. The fields for each element are calculated by subtracting maximum and minimum changes in base metal concentration during alteration (Table 2) from modeled protolith curves determined using the coefficients given in Table 1. The diagram indicates that protolith differentiation is a potentially important control on the release of base metals into hydrothermal fluids during alteration.

ACCEPTED MANUSCRIPT

Tables

Table 1. Coefficients used in modeling protolith base metal contents (Eq. 1) based on differentiation curves defined by new analyses of Troodos glasses (Fig. 2). The RMSD values give an indication of the fit of the model to the data (Eq. 2).

| Element (ppm) | A | B | RMSD |
|---------------|--------|---------|-------|
| Mn | 505.8 | 0.2580 | 174.1 |
| Cu | 779.2 | -0.9428 | 11.2 |
| Co | 69.5 | -0.3340 | 6.6 |
| Ni | 4722.6 | -1.6460 | 6.6 |
| Zn | 8.1 | 0.6372 | 14.5 |

Table 2. Change (Δ) in base metal concentration from their protolith for samples from each alteration facies within the Spilia–Kannavia epidosite zone, where negative numbers indicate metal loss and positive numbers indicate metal gain during alteration. Max = Maximum loss of base metal, Min = Minimum loss, Av = Average loss, SD = standard deviation and n = number of samples.

| Facies | | Δ M Zn | % | Δ M Ni | % | Δ M Mn | % | Δ M Co | % | Δ M Cu | % |
|-------------------------------|-----|---------------|-----|---------------|-----|---------------|-----|---------------|-----|---------------|-----|
| | | ppm | |
| Diabase n=61 | Min | -23.6 | -38 | 34.3 | 233 | 213 | 20 | 47.4 | 220 | -7.0 | -28 |
| | Max | -78.2 | -97 | -35.1 | -92 | -1070 | -83 | -18.4 | -71 | -55.0 | -97 |
| | Av | -54.1 | -78 | -3.8 | -18 | -407 | -32 | 12.7 | 56 | -32.2 | -91 |
| | SD | 15.2 | 13 | 9.8 | 54 | 359 | 29 | 9.6 | 42 | 10.5 | 10 |
| Trans. diab–epidosite n=26 | Min | -44.2 | -59 | -3.2 | -26 | -332 | -27 | 30.0 | 144 | -14.8 | -70 |
| | Max | -88.2 | -95 | -11.9 | -79 | -1071 | -84 | -4.9 | -25 | -30.1 | -94 |
| | Av | -65.4 | -80 | -7.4 | -59 | -671 | -52 | 11.1 | 53 | -23.3 | -90 |
| | SD | 10.1 | 9 | 2.2 | 14 | 159 | 12 | 8.8 | 41 | 3.9 | 6 |
| Intermed. epidosite n=31 | Min | -45.7 | -73 | -3.7 | -15 | -332 | -29 | 14.5 | 66 | -20.9 | -60 |
| | Max | -78.4 | -95 | -21.1 | -88 | -1073 | -84 | -4.8 | -24 | -35.2 | -95 |
| | Av | -63.5 | -84 | -10.3 | -68 | -655 | -52 | 5.9 | 27 | -26.6 | -91 |
| | SD | 8.9 | 6 | 3.9 | 18 | 176 | 13 | 5.8 | 27 | 4.4 | 6 |
| End-member epidosite n=18 | Min | -45.6 | -76 | -5.5 | -65 | -375 | -34 | 4.1 | 16 | 2.0 | 5 |
| | Max | -86.9 | -96 | -24.2 | -88 | -897 | -75 | -18.4 | -82 | -42.7 | -97 |
| | Av | -65.4 | -91 | -14.5 | -78 | -734 | -60 | -6.4 | -29 | -27.5 | -87 |

SD 11.7 6 5.5 7 143 10 5.6 25 10.3 24

Table 3. Average base metal contents (ppm) in each alteration facies compared to the average protolith. *Note that these averages were not used in the mass balance calculations and are given for comparative purposes only.*

| | Protolith at average altered rock Y | Diabase | Transitional Diabase– epidosite | Intermediate epidosite | End-member epidosite |
|-----------|---|---------|---------------------------------------|---------------------------|-------------------------|
| Average Y | 31.8 | 28.9 | 37.7 | 33.3 | 30.8 |
| n | 136 | 61 | 26 | 31 | 18 |
| Mn | 1235 | 789 | 616 | 592 | 485 |
| Zn | 73.7 | 14.6 | 16.4 | 12.1 | 6.3 |
| Ni | 15.9 | 18.4 | 5.3 | 5.3 | 4.0 |
| Co | 21.9 | 35.7 | 31.8 | 27.6 | 15.9 |
| Cu | 29.8 | 3.0 | 2.5 | 2.8 | 4.4 |

Table 4. Volume, density and mass of altered rock and amount of base metal released during hydrothermal alteration for individual lithologies within the Spilia–Kannavia epidosite zone. Note that whilst values have been calculated for Co it is likely that no Co was removed from the epidosite zone. Errors were estimated as follows. Uncertainties in the fraction of diabase and epidosite alteration facies were determined from counting statistics of field observation of >200 dikes (10% relative). This uncertainty was applied to the proportions of the four sub-facies. Analytical precision for the bulk-rock base metals (Mn: 3.5%; Cu: 7%; Co: 5.4%; Ni: 6.12%; Zn: 5.2% and Y: 16%) and the uncertainty on the fit of the glass data to Eq. 1 (RMSD, Table 1) were propagated into an uncertainty on the change in base metal content for each sample. The uncertainty in the average change in metal content for each alteration facies includes both the analytical uncertainties on each sample and the standard deviation in the change in metal content of all samples, which is much larger and incorporates the natural variation of the samples (Table 2). The accuracy of the LA–ICP–MS glass analyses was estimated from analysis of NIST 612 (Cu: 25%; Co: 19%; Ni: 12.5%; Zn: 26%) and these uncertainties were propagated linearly into the overall uncertainty. Note that the errors below ignore the constraint of constant sum to 100% for percentages of the different facies – Monte Carlo modeling incorporating this constraint indicates that taking this into account would reduce the errors below for metal loss by between ~50% (Zn) and 4% (Mn).

| Facies | Volume % (±) | Volume km ³ (±) | Density kg m ⁻³ | Mass Mt (±) | Zn kt (±) | Ni kt (±) | Mn kt (±) | Co kt (±) | Cu kt (±) |
|-----------------------|-----------------|-------------------------------|-------------------------------|----------------|--------------|--------------|--------------|--------------|--------------|
| Diabase | 23.6 (2.4) | 0.47 (0.05) | 2847 | 1346 (135) | 73 (34) | 5 (14) | 548 (488) | -17 (14) | 43 (18) |
| Trans. diab–epidosite | 24.4 (2.4) | 0.49 (0.05) | 2847 | 1387 (139) | 91 (32) | 10 (5) | 930 (245) | -15 (14) | 32 (13) |
| Int. epidosite | 39.4 (3.9) | 0.79 (0.08) | 3095 | 2438 (244) | 155 (55) | 25 (11) | 1596 (465) | -14 (18) | 65 (23) |
| E.M. epidosite | 12.6 (1.3) | 0.25 (0.03) | 3095 | 780 (78) | 51 (19) | 11 (5) | 572 (130) | 5 (6) | 21 (10) |
| Total | 100.0 | 2.00 | | 5952 (321) | 369 (74) | 52 (19) | 3647 (729) | -42 (27) | 162 (34) |

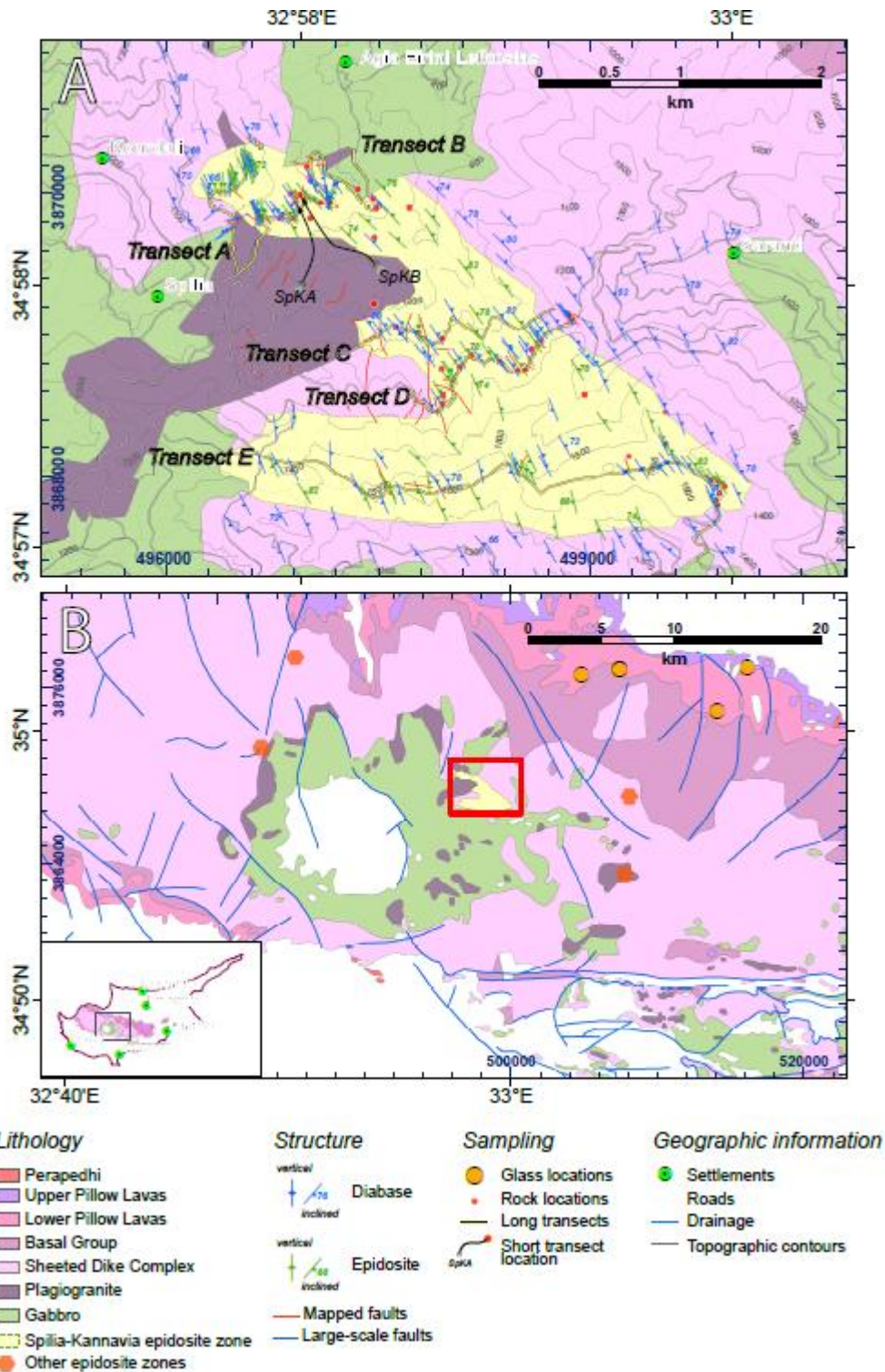


Figure 1

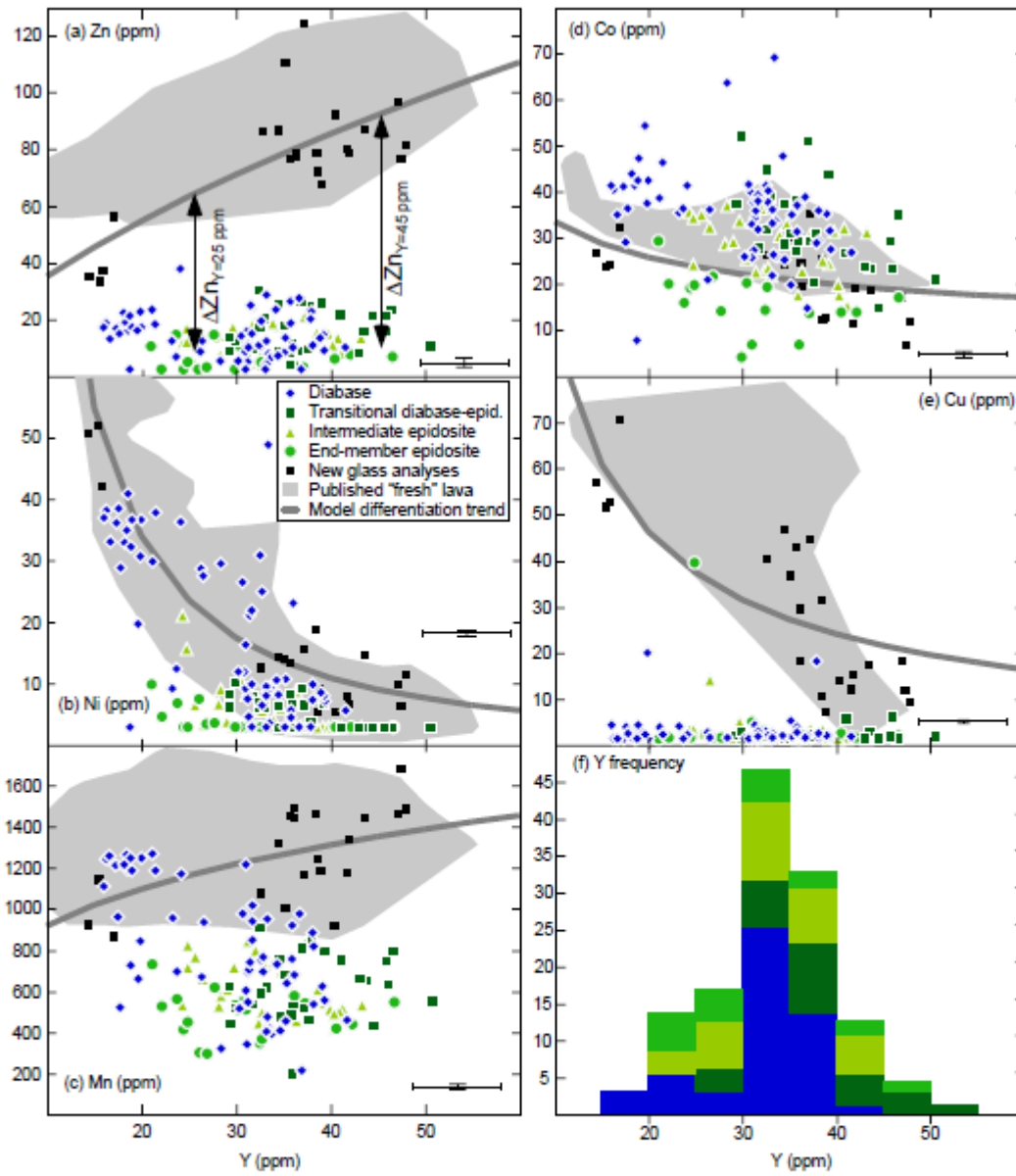


Figure 2

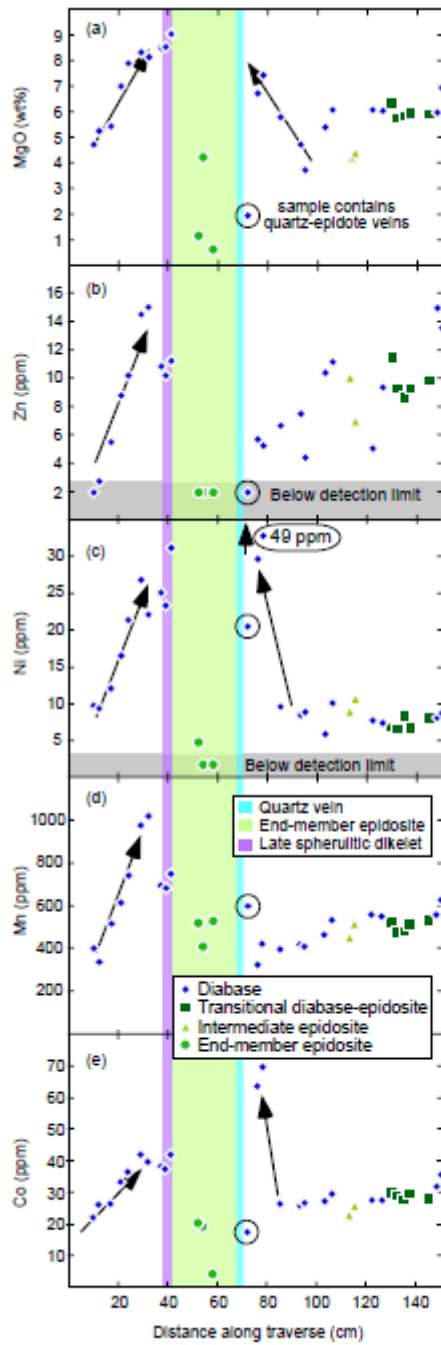


Figure 3

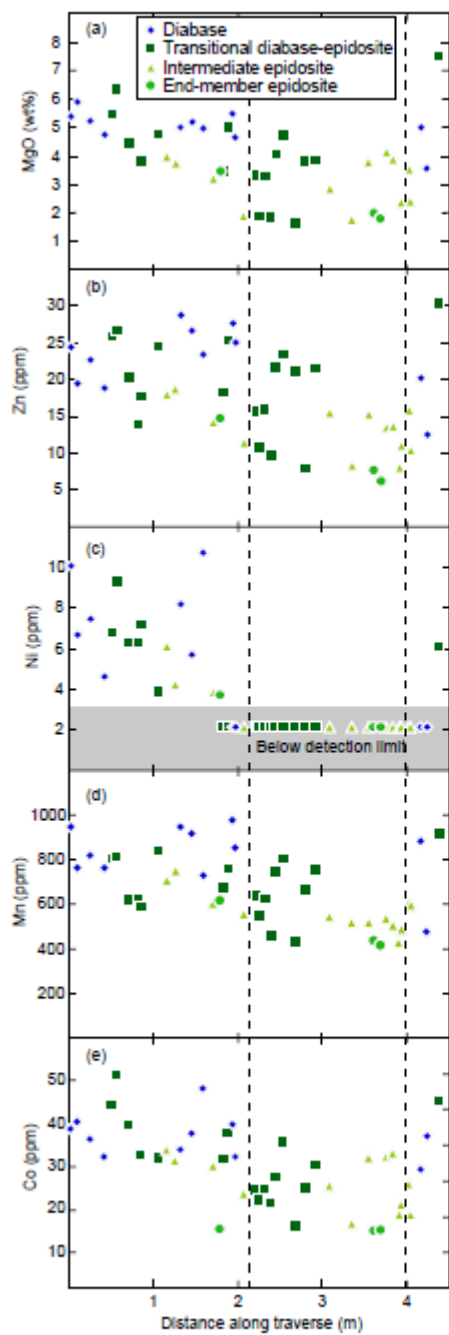


Figure 4

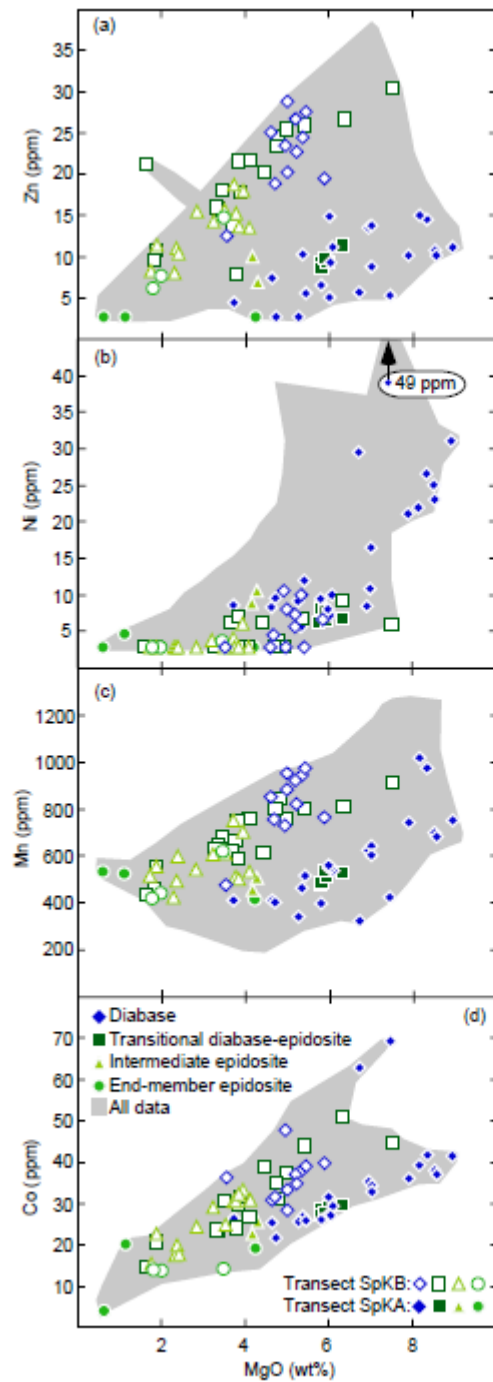


Figure 5

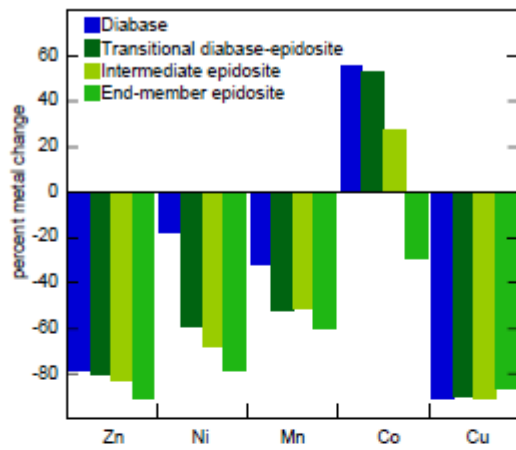


Figure 6

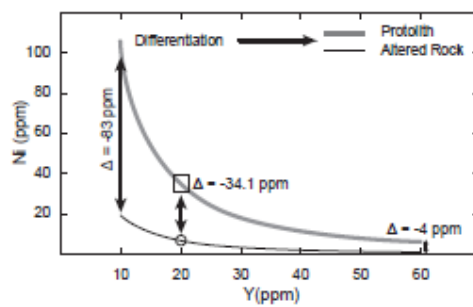


Figure 7

ACCEPTED

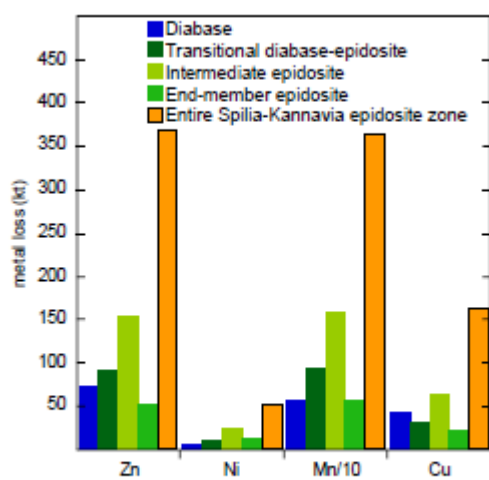


Figure 8

A

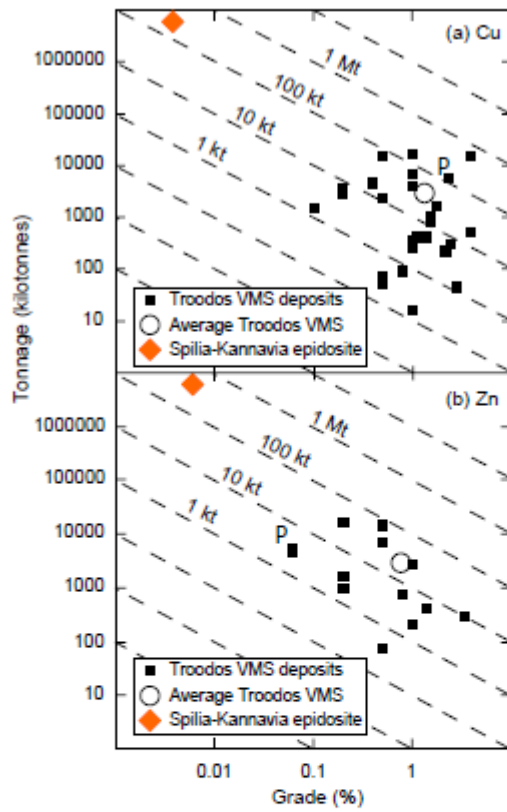


Figure 9

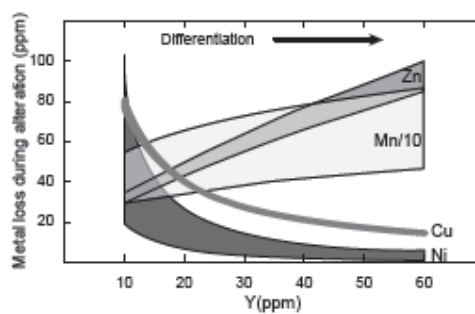


Figure 10

ACCEPTED

Highlights

- Protolith differentiation key in quantifying metal losses from sheeted dike complex
- Altering primitive protoliths gives high Cu + Ni: Zn + Mn fluids; evolved opposite
- All Cu and most Zn is leached from all rocks irrespective of alteration mineralogy
- No Co and little Mn and Ni is lost during chlorite-amphibole alteration
- Metal losses could have formed a large high grade Troodos VMS deposit

ACCEPTED MANUSCRIPT